Received June 5, 2019, accepted June 30, 2019, date of publication July 3, 2019, date of current version July 17, 2019.

Digital Object Identifier 10.1109/ACCESS.2019.2926516

Vibration Control of a Flexible Spacecraft System With Input Backlash

ZHIQIANG LIN[1], SHIMIN LIN[2], SEN WU[3], GE MA[3], AND ZHONGWEI LIANG[3]

[1]School of Mathematics and Information Science, Guangzhou University, Guangzhou 510006, China
[2]Jacobs School of Engineering, University of California at San Diego, La Jolla, CA 92037, USA
[3]School of Mechanical and Electrical Engineering, Guangzhou University, Guangzhou 510006, China

Corresponding author: Ge Ma (m_ge@gzhu.edu.cn)

This work was supported in part by the National Natural Science Foundation of China under Grant 61803110, in part by the Natural Science Foundation of Guangdong Province, China, under Grant 2018A030310065, in part by the Science and Technology Innovative Research Team Program in Higher Educational Universities of Guangdong Province under Grant 2017KCXTD025, and in part by the Innovative Academic Team Project of Guangzhou Education System under Grant 1201610013.

ABSTRACT In this paper, we deal with the vibration control problem of a flexible spacecraft system with unknown external disturbance and uncertain input backlash nonlinearity. The considered system is described by two partial differential equations and an ordinary differential equation as governing equations, and by ordinary differential equations as boundary conditions. The backlash nonlinearity is reformulated into the desired control input associated with an extra input nonlinear error. This input error and the external disturbance are combined into an unknown ‘‘disturbance-like’’ item. Two boundary control inputs are designed at the center body of the spacecraft, compensating for the unknown upper-bound of such items by applying proper online updating laws. As a result, the vibration of both solar panels of the flexible spacecraft is suppressed and their angle positions are regulated in the desired region. The numerical simulations are provided to verify the control performance of the proposed controls by the choice of proper parameters.

INDEX TERMS Vibration control, adaptive control, flexible satellite, input backlash.

I. INTRODUCTION

Nonsmooth input nonlinearities often occur in real control for industrial implementation, including saturation, backlash, hysteresis and dead-zone [1], [2]. Actually, the ignorance of these nonlinear characteristics in control system design will deteriorate the system performance [3], [4]. Many studies and methodologies have sought to handle these constraints [5], [6]. The backlash nonlinearity, which is a clearance or lost motion in a mechanism caused by gaps between the parts, is usually poorly known and often limits system performance [7]. Neglecting input backlash may result in serious instability [8], [9]. Unfortunately, most traditional control schemes are not effective enough to handle systems with backlash, since backlash is non-differentiable, non-linearities and usually unknown characteristic. Several new modeling methods on backlash pattern and control techniques have recently been proposed, e.g., phase plane model [10], dead-zone model [11], and neural network-based control [12]. In [13], the PrandtlCIshinskii hysteresis operator is adopted to eliminate the effect of the input backlash. In [14], a novel integral control method is proposed for the systems with the input and the output hysteresis. In [15], an output feedback method is applied to design a controller to deal with the feedback signals which cannot be measured directly, thus the backlash nonlinearity is handled.

Spacecrafts with flexible solar panels have received increasing attention in communication, remote sensing and space industry, because the flexible structures are able to adapt many complex application environments. However, undesirable vibration caused by the flexible property is a thorny problem. Thus, a number of approaches have been proposed for designing controllers to suppress the vibration, such as positive position control [16], neural network control [17], optimal control [18], sliding mode control [8], [19], linear quadratic regulator control [20], etc. Most of these studies are based on finite dimensional ordinary differential equations (ODEs) models [21], [22]. However, flexible structures are close to infinite dimensional systems from a mathematical point of view [23], [24].

The associate editor coordinating the review of this manuscript and approving it for publication was Jianyong Yao.

Hence dimensionality reductions may lead to spill over instability [25], [26].

In order to solve the aforementioned issue, original infinite dimensional partial differential equations (PDEs) are adopted to describe the flexible structures [27], [28]. Boundary control technology has been proposed based on the PDEs model [29], [30]. An advantage of this technology is that the implementation only necessary to set up actuators and sensors at the boundaries [31], [32]. In [33], a robust adaptive boundary control for an axially moving string is investigated, by applying a hydraulic actuator at the right boundary of the string. In [34], the stabilization of a Timoshenko beam with a tip payload subjected to boundary external disturbances is considered. The effects of the external disturbances have been eliminated according to design some nonlinear feedback control laws. In [35], an uncertainty and disturbance estimator based robust boundary control strategy is presented, to handle the stabilization of an unstable parabolic partial differential equation with unknown input disturbance.

Literature [36] first proposes a boundary control scheme based on hybrid PDEs-ODEs model for a flexible satellite. A single-point control input is placed at the hub to restrain the vibrations of the two panels. In [37], the flexible spacecraft system subjected to external disturbances is investigated. An efficient control scheme consisting of two boundary control laws and a distributed control law is developed to suppress the vibration and track the desired attitude. In [38], by setting up a control torque in the central hub of the flexible spacecraft system, the exponential stabilization of the closed-loop system is achieved. With regard to the research of input constraints of the flexible spacecraft system, although input saturation phenomenon has been taken into account in [39], [40], to the best of our knowledge, there is not any published literature attempting to design boundary control scheme for flexible spacecraft with input backlash. Hence it motivates us to carry out this research.

In this paper, we consider the vibration control problem of a flexible spacecraft system with unknown external disturbance and uncertain input backlash non-linearity. The studied system is described by a set of PDEs and ODEs. We define an appropriate Lyapunov function candidate and design a novel boundary control scheme with considering the unknown external disturbance and the uncertain input backlash non-linearity in the system. Different from the previous existing research studies, main contributions of this paper can be summed up as follows:

- *i* The input backlash is presented as a desired control input associated with an input non-linear error. The input non-linear error and external disturbance form an unknown 'disturbance-like' item.
- *ii* A novel boundary control scheme is presented, including two control inputs. Based on applying proper online updating laws, the unknown upper-bound of the 'disturbance-like' items can be estimated.

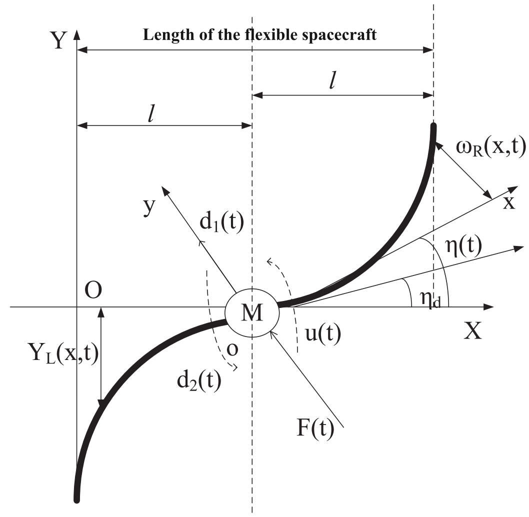

FIGURE 1. **A typical flexible spacecraft system [39].**

- *iii* With the proposed controls, the vibration of the flexible spacecraft is suppressed and the angle position is regulated in the desired region. Moreover, the closed-loop system is proved to be uniformly bounded via the Lyapunovs direct method.

The arrangement of this paper is listed as below. A PDEs-ODEs model of the flexible spacecraft system and preliminaries are presented in Section II. Considering the input backlash non-linearity and the boundary external disturbances, a novel boundary control algorithm is proposed in Section III. Numerical simulations are completed in Section IV and we reach a conclusion in Section V.

II. PROBLEM STATEMENT AND PRELIMINARIES

In this paper, we directly use the system model described in [39], which is proposed for investigating the input saturation issue of the flexible spacecraft system. We will handle the input backlash problem for this model.

As is shown in Fig. 1, the frame consists of a inertial coordinate XOY and a fixed coordinate xoy. $\omega_L(x, t)$ and $\omega_R(x, t)$ are the deflections in xoy of the left and right panels, respectively. The displacements of the two panels in XOY are denoted as

$$\begin{cases} Y_L(x,t) = \omega_L(x,t) + l\eta(t) \\ Y_R(x,t) = \omega_R(x,t) + l\eta(t). \end{cases} \quad (1)$$

$\eta(t)$ represents the attitude angle displacement, and η_d is the desired angle displacement. M denotes the point mass of the center body. The length of the symmetrical flexible panel is l. I_h is the center body inertia. $\bar{d}_1(t)$ and $\bar{d}_2(t)$ denote the external input disturbances, while $u(t)$ and $F(t)$ are the corresponding control inputs. ρ is the density of the panels. γ_1 is the coefficient of viscous damping. EI is the bending stiffness.

Remark 1: For convenience and clarity, notions $(\star)' = \partial(\star)/\partial x$, $(\star)'' = \partial^2(\star)/\partial x^2$, $(\star)''' = \partial^3(\star)/\partial x^3$, $(\star)^{(n)} =$

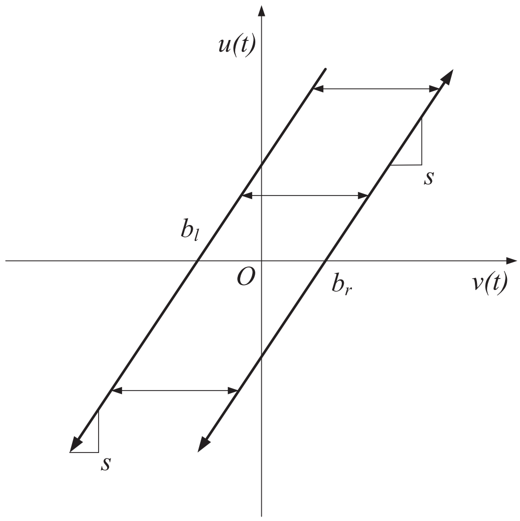

FIGURE 2. Diagram of backlash.

$\partial^n(\star)/\partial x^n$ $(n \geq 4)$, $(\dot{\star}) = \partial(\star)/\partial t$, and $(\ddot{\star}) = \partial^2(\star)/\partial t^2$ are defined throughout this paper.

The flexible spacecraft system proposed in [39] are described with three governing equations:

$$\begin{cases} \rho\ddot{Y}_L(x,t) + EIY_L^{(4)}(x,t) + \gamma_1\dot{Y}_L(x,t) = 0, \\ x \in (0,l), \qquad t > 0 \\ \\ \rho\ddot{Y}_R(x,t) + EIY_R^{(4)}(x,t) + \gamma_1\dot{Y}_R(x,t) = 0, \\ x \in (l,2l), \qquad t > 0 \end{cases} \tag{2}$$

and

$$I_h\ddot{\eta}(t) = EI[Y_R''(l,t) - Y_L''(l,t)] + u(t) + \bar{d}_1(t), \quad t > 0 \tag{3}$$

where $u(t)$ is the axial control force and $\bar{d}_1(t)$ is the external input disturbance.

The corresponding boundary conditions are:

$$\begin{cases} Y_L(l,t) = Y_R(l,t) = Y(l,t), & t \geq 0 \\ Y_L''(0,t) = Y_L'''(0,t) = 0, & t \geq 0 \\ Y_R''(2l,t) = Y_R'''(2l,t) = 0, & t \geq 0 \end{cases} \tag{4}$$

and

$$M\ddot{Y}(l,t) = EI[Y_L'''(l,t) - Y_R'''(l,t)] + F(t) + \bar{d}_2(t), \quad t \geq 0 \tag{5}$$

where $F(t)$ is the control torque and $\bar{d}_2(t)$ is the external input disturbance.

From the boundary conditions (4) and the equations (1), we have $Y_L'(l,t) = Y_R'(l,t) = \eta(t)$. And we also have $Y_L^{(n)}(x,t) = \omega_L^{(n)}(x,t)$, $Y_R^{(n)}(x,t) = \omega_R^{(n)}(x,t)$, $n \geq 2$.

As is shown in Fig 2, The input backlash proposed in [1] is reformulated as follows

$$u(t) = B(\nu) = s\nu(t) + d(\nu) \tag{6}$$

where $u(t)$ denotes the control input, $\nu(t)$ denotes the desired control command, $s > 0$ is the slope, $d(\nu)$ is the non-linearity error and has the below expression

$$d(\nu) = \begin{cases} -sb_r, & \text{if } \dot{\nu} > 0 \text{ and } u(t) = s(\nu(t) - b_r) \\ -sb_l, & \text{if } \dot{\nu} < 0 \text{ and } u(t) = s(\nu(t) - b_l) \\ u(t\_) - s\nu(t) & \text{otherwise}, \end{cases} \tag{7}$$

in which $b_l < b_r$ are constant parameters and $u(t\_)$ means there is no change of $u(t)$.

Several necessary assumptions are proposed for the subsequent development.

Assumption 1: The backlash output $B(\nu)$ is hard to measure.

Assumption 2: The parameters s, b_r and b_l are unknown bounded constants. However, their signs are specific such that $s > 0$, $b_r > 0$ and $b_l < 0$. Moreover, they are within known bounded

$$0 < s_{min} \leq s \leq s_{max}, \tag{8}$$

$$0 < (b_r)_{min} \leq b_r \leq (b_r)_{max}, \tag{9}$$

$$(b_l)_{min} \leq b_l \leq (b_l)_{max} < 0. \tag{10}$$

Assumption 3: The unknown external input disturbances $\bar{d}_1(t)$ and $\bar{d}_2(t)$ are also bounded.

Under these assumptions, we have

$$|d(\nu)| \leq \max\{sb_r, -sb_l\}.$$

And we define the 'disturbance-like' term as

$$d(t) = d(\nu) + \bar{d}(t). \tag{11}$$

Remark 2: The following inequality presented in [41] will be applied for analyzing the system stability.

$$|y(l,t)D(t)| \leq y(l,t)\tanh(y(l,t))D_m, \tag{12}$$

where $\tanh(*)$ denotes the hyperbolic tangent function and $D_m > \max\{|D(t)|\} > 0$.

III. ADAPTIVE CONTROL DESIGN

Different from the dynamics of robotic manipulator or marine riser represented by a single governing PDE equation, the flexible spacecraft system is represented by two PDE equations and more complex boundary conditions. Furthermore, the control goals of this study are to suppress the vibration and to restrict the angle position, while the previous controls in [15], [42] are only for the stability. Hence the previous methods proposed in [15], [42] cannot directly apply to this study without difficulty.

In this section, an extension of backlash handling approaches to the flexible spacecraft system is presented. In order to stabilize the system and compensate for the "disturbance-like" terms, the boundary controls $F(t)$ and $u(t)$ are designed based on the Lyapunov's direct method. Our control designs will make sure that all the states of the closed-loop system are uniformly ultimately bounded.

The input backlash models of the flexible spacecraft system can be described as follows

$$u(t) = B_u(\nu) = s\nu(t) + d_1(\nu) \tag{13}$$

and

$$F(t) = B_F(\sigma) = g\sigma(t) + d_2(\sigma) \tag{14}$$

where $\nu(t)$ and $\sigma(t)$ are the two designed boundary control inputs. s and g are the positive constant slope of the lines associated with $\nu(t)$ and $\sigma(t)$, respectively.

According to (7), the non-linearity errors $d_1(t)$ and $d_2(t)$ can be formulated as

$$d_1(\nu) = \begin{cases} -sb_{ur}, & \text{if } \dot{\nu} > 0 \text{ and } u(t) = s(\nu(t) - b_{ur}) \\ -sb_{ul}, & \text{if } \dot{\nu} < 0 \text{ and } u(t) = s(\nu(t) - b_{ul}) \\ u(t\_) - s\nu(t) & \text{otherwise} \end{cases} \tag{15}$$

and

$$d_2(\sigma) = \begin{cases} -gb_{Fr}, & \text{if } \dot{\sigma} > 0 \text{ and } F(t) = g(\sigma(t) - b_{Fr}) \\ -gb_{Fl}, & \text{if } \dot{\sigma} < 0 \text{ and } F(t) = g(\sigma(t) - b_{Fl}) \\ F(t\_) - g\sigma(t) & \text{otherwise.} \end{cases} \tag{16}$$

Then the governing equation (3) and the boundary condition (5) can be rewritten as

$$I_h\ddot{\eta}(t) - EI[Y_R''(l,t) - Y_L''(l,t)] = s\nu(t) + d_1(t), \tag{17}$$
$$M\ddot{Y}(l,t) - EI[Y_L'''(l,t) - Y_R'''(l,t)] = g\sigma(t) + d_2(t) \tag{18}$$

where

$$d_1(t) = d_1(\nu) + \bar{d}_1, \tag{19}$$
$$d_2(t) = d_2(\sigma) + \bar{d}_2 \tag{20}$$

are the 'disturbance-like' terms. Since $d_1(\nu)$, $\bar{d}_1$, $d_2(\sigma)$ and $\bar{d}_2$ are bounded, $d_1(t)$ and $d_2(t)$ are bounded within unknown positive constant $\mathcal{D}$ and $\mathcal{Q}$, respectively. We will estimate $\mathcal{D}$ and $\mathcal{Q}$ later.

The desired control inputs are presented as follows

$$\nu(t) = \frac{1}{s}[-k_1\dot{e} - k_2 e - \tanh(h(t))\hat{\mathcal{D}}(t)] \tag{21}$$
$$\sigma(t) = \frac{1}{g}[-ku_a(t) - \frac{m\beta}{\alpha}\dot{\omega}(l,t) - k_d\omega(l,t) - \tanh(u_a(t))\hat{\mathcal{Q}}(t)] \tag{22}$$

where $k, k_1, k_2, k_d, \alpha, \beta$ are positive constants, $\hat{\mathcal{D}}(t)$ and $\hat{\mathcal{Q}}(t)$ are the observers of $\mathcal{D}$ and $\mathcal{Q}$, respectively. Then the errors of estimation of $\mathcal{D}$ and $\mathcal{Q}$ can be defined as $\tilde{\mathcal{D}}(t) = \mathcal{D} - \hat{\mathcal{D}}(t)$ and $\tilde{\mathcal{Q}}(t) = \mathcal{Q} - \hat{\mathcal{Q}}(t)$, respectively. Hence we have $\dot{\tilde{\mathcal{D}}}(t) = -\dot{\hat{\mathcal{D}}}(t)$ and $\dot{\tilde{\mathcal{Q}}}(t) = -\dot{\hat{\mathcal{Q}}}(t)$. The adaptive laws are expressed as

$$\dot{\hat{\mathcal{D}}}(t) = h(t)\tanh(h(t)) - \xi_1\hat{\mathcal{D}}(t), \tag{23}$$
$$\dot{\hat{\mathcal{Q}}}(t) = \alpha u_a(t)\tanh(u_a(t)) - \xi_2\hat{\mathcal{Q}}(t) \tag{24}$$

where ξ_1 and ξ_2 are positive constants. Moreover, $h(t)$ and $u_a(t)$ are expressed as

$$h(t) = \alpha\dot{e} + \beta e \tag{25}$$

and

$$u_a(t) = \dot{\omega}(l,t) + \frac{\beta}{\alpha}\omega(l,t), \tag{26}$$

respectively, in which

$$e = \eta(t) - \eta_d \tag{27}$$

and it implies that $\dot{e} = \dot{\eta}(t)$.

Remark 3: *In the designed control laws* (21) *and* (22)*, all signals can be measured by sensors located at the center body or computed by backward difference algorithm. We can directly measure* $\omega(l,t)$ *by applying a laser displacement sensor, and use the backward difference algorithm to calculate* $\dot{\omega}(l,t)$ *according to the measured value.* $\eta(t)$ *and* $\dot{\eta}(t)$ *can be measured by employing a rotary encoder and tachometer, respectively. Although measurement noises objectively exist in sensors' implementation, the effect is obvious for the high order differentiating terms with respect to time and weak for first-order differentiating terms. In the proposed controls* (21) *and* (22)*, only* $\dot{\omega}(l,t)$ *and* $\dot{\eta}(t)$ *with differentiating once exist, thus the effects of the noises can be ignored in practice.*

The Lyapunov function candidate of our chosen is

$$\mathcal{V}(t) = \mathcal{V}_a(t) + \mathcal{V}_b(t) + \mathcal{V}_c(t) + \frac{1}{2}\tilde{\mathcal{D}}^2(t) + \frac{1}{2}\tilde{\mathcal{Q}}^2(t) \tag{28}$$

where $\mathcal{V}_a(t)$, $\mathcal{V}_b(t)$ and $\mathcal{V}_c(t)$ are defined as

$$\begin{aligned} \mathcal{V}_a(t) \,| =& \frac{\alpha EI}{2}\int_0^l [\omega_L''(x,t)]^2 dx + \frac{\alpha EI}{2}\int_l^{2l} [\omega_R''(x,t)]^2 dx \\ &+ \frac{\beta\gamma_1}{2}\int_0^l Y_{L_e}^2(x,t)dx + \frac{\beta\gamma_1}{2}\int_l^{2l} Y_{R_e}^2(x,t)dx \\ &+ \frac{\alpha\rho}{2}\int_0^l \dot{Y}_L^2(x,t)dx + \frac{\alpha\rho}{2}\int_l^{2l} \dot{Y}_R^2(x,t)dx, \end{aligned} \tag{29}$$

$$\mathcal{V}_b(t) = \frac{\alpha m}{2}u_a^2(t) + \frac{\alpha k_d}{2}\omega^2(l,t) + (\frac{\alpha k_2}{2} + \frac{\beta k_1}{2})e^2 + \frac{\alpha I_h}{2}\dot{e}^2, \tag{30}$$

$$\mathcal{V}_c(t) = \beta I_h e\dot{e} + \beta\rho\int_0^l \dot{Y}_L(x,t)Y_{L_e}(x,t)dx + \beta\rho\int_l^{2l} \dot{Y}_R(x,t)Y_{R_e}(x,t)dx \tag{31}$$

where $Y_{L_e}(x,t) = \omega_L(x,t) + xe$ and $Y_{R_e}(x,t) = \omega_R(x,t) + xe$.

Lemma 1: *The Lyapunov function candidate* (28) *is a positive function and is upper and lower bounded as*

$$\begin{aligned} 0 &\le \lambda_1[\mathcal{V}_a(t) + \mathcal{V}_b(t) + \tilde{\mathcal{D}}^2(t) + \tilde{\mathcal{Q}}^2(t)] \le \mathcal{V}(t) \\ &\le \lambda_2[\mathcal{V}_a(t) + \mathcal{V}_b(t) + \tilde{\mathcal{D}}^2(t) + \tilde{\mathcal{Q}}^2(t)] \end{aligned} \tag{32}$$

where λ_1 *and* λ_2 *are two positive constants.*

Proof: Please see Appendix A. □

Lemma 2: *The time derivative of the Lyapunov function candidate* (28) *can be upper bounded with*

$$\dot{\mathcal{V}}(t) \le -\lambda\mathcal{V}(t) + \varepsilon \tag{33}$$

where $\lambda > 0$ *and* $\varepsilon > 0$.

Proof: Please see Appendix B. □

Theorem 1: For the studied flexible spacecraft system described by (2)-(5), under the proposed control laws (21) and (22) with suitable parameters, assuming that the initial conditions are bounded, the closed-loop system is uniformly bounded.

Proof: Multiplying (33) by $exp(\lambda t)$, and integrating the consequence yields

$$\mathcal{V}(t) \leq \mathcal{V}(0)exp(-\lambda t) + \frac{\varepsilon}{\lambda} \in \mathcal{L}_\infty. \quad (34)$$

We further have

$$\begin{cases} \omega_L^2(x,t) \leq (2l+1)\omega^2(l,t) + (l+16l^4)\int_0^l [\omega_L''(x,t)]^2 dx \\ \omega_R^2(x,t) \leq (2l+1)\omega^2(l,t) + (l+16l^4)\int_0^l [\omega_R''(x,t)]^2 dx \end{cases} \quad (35)$$

By Lemma 1, (29) and (30), we can further obtain

$$\begin{cases} \omega_L^2(x,t) \leq \tau[\mathcal{V}_a(t) + \mathcal{V}_b(t)] \leq \frac{\tau}{\lambda_2}\mathcal{V}(t) \\ \omega_R^2(x,t) \leq \tau[\mathcal{V}_a(t) + \mathcal{V}_b(t)] \leq \frac{\tau}{\lambda_2}\mathcal{V}(t) \end{cases} \quad (36)$$

where $\tau = \max\{\frac{4l+2}{\alpha k_d}, \frac{2l+32l^4}{\alpha EI}\} > 0$.

Substituting (34) into (36), we get

$$\begin{cases} |\omega_L(x,t)| \leq \sqrt{\frac{\tau}{\lambda_2}[\mathcal{V}(0) + \frac{\varepsilon}{\lambda}]}, \quad \forall (x,t) \in [0,l] \times [0,\infty), \\ |\omega_R(x,t)| \leq \sqrt{\frac{\tau}{\lambda_2}[\mathcal{V}(0) + \frac{\varepsilon}{\lambda}]}, \quad \forall (x,t) \in [l,2l] \times [0,\infty) \end{cases} \quad (37)$$

In the same manner, we have

$$|e| = |\eta(t) - \eta_d| \leq \sqrt{\frac{\vartheta}{\lambda_2}[\mathcal{V}(0) + \frac{\varepsilon}{\lambda}]}, \quad \forall t \in [0,\infty) \quad (38)$$

where $\vartheta = 2/(\alpha k_2 + \beta k_1)$. Hence, we can obtain

$$\lim_{t\to\infty} |\omega_L(x,t)| \leq \sqrt{\frac{\tau\varepsilon}{\lambda\lambda_2}}, \quad \lim_{t\to\infty} |\omega_R(x,t)| \leq \sqrt{\frac{\tau\varepsilon}{\lambda\lambda_2}} \quad (39)$$

and

$$\lim_{t\to\infty} |e| \leq \sqrt{\frac{\vartheta\varepsilon}{\lambda\lambda_2}}. \quad (40)$$

□

Remark 4: A reasonable selection process of the control design parameters can make sure that constraint conditions (60)-(64) are satisfied. Since J is neither a design parameter nor a system parameter, J can be assigned an arbitrary value. It implies that we can first choose a proper β, and determine J according to (61). Then α can be selected by (60). k_d, k_1 and k_2 are chosen for making (62), (63) and (64) hold, respectively. In simulations, we will repeat the above parameters selection procedure, until better control performances are achieved.

TABLE 1. Parameters of the flexible spacecraft system.

Parameter	Description	Value
l	Length of the solar panel	10m
M	Point mass of the center body	100kg
EI	Bending stiffness of the spacecraft	1.2×10^3Nm^2
γ_1	Coefficient of viscous damping	600kg/(ms)
ρ	Mass of the unit length	54kg/m
I_h	Inertia of center body	500kg/m

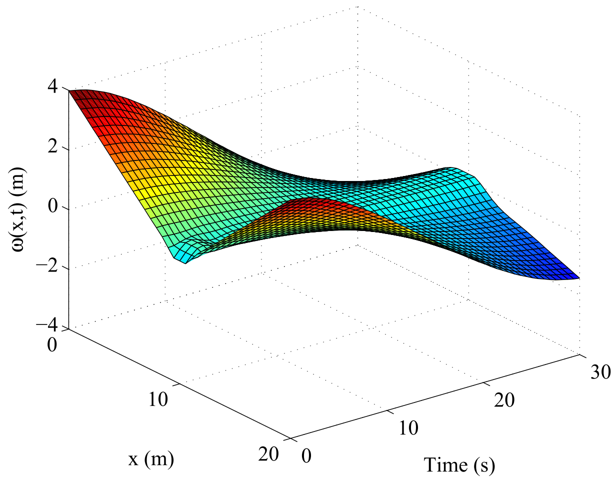

FIGURE 3. Deflection of the uncontrolled spacecraft.

IV. SIMULATIONS

In order to verify the effectiveness of our proposed control scheme for the flexible spacecraft system with input backlash non-linearity, simulations have been carried out by using the finite difference method [24], [43] and the results are presented in this section.

The finite difference method can provide a straightforward and accurate process to resolve the dynamic model (2)-(5) constituting a highly nonlinear and hybrid differential equations with two independent variables, i.e., space and time. The space step and the time step are divided as $\Delta x = 0.5$m and $\Delta t = 3 \times 10^{-4}$s, respectively. The spatial and temporal terms in the equations are obtained using the finite difference techniques through a finite rectangular grid on this mesh of discrete points.

The parameters of the considered system are shown in Table 1. The boundary disturbance and initial conditions of the system are as follows $\bar{d}_1(t) = \bar{d}_2(t) = 1.2 + \sin(\pi t)$, $\omega_L(x,0) = \omega_R(x,0) = 0.2x$, $\dot{\omega}_L(x,0) = \dot{\omega}_R(x,0) = 0$, $\eta(0) = 0(rad)$ and $\eta_d = 0.5(rad)$.

Without any control input, i.e. $u(t) = F(t) = 0$, the deflection is always large as shown in Fig. 3. From Fig. 5, we can see that the angle displacement of the spacecraft is less than 0.3 rad, which exceeds the desired position $\eta_d = 0.5$ rad.

Boundary control laws (13) and (14) are executed by setting $k_d = 50$, $k = 100$, $k_1 = 300$, $k_2 = 800$, $\alpha = 1.2$, $\beta = 0.6$, $\xi_1 = 0.001$ and $\xi_2 = 0.08$. $s = g = 1$, $b_{ul} = -50$, $b_{ur} = 50$, $b_{Fl} = -10$ and $b_{Fr} = 10$ are chosen as the parameters of the input backlash non-linearity.

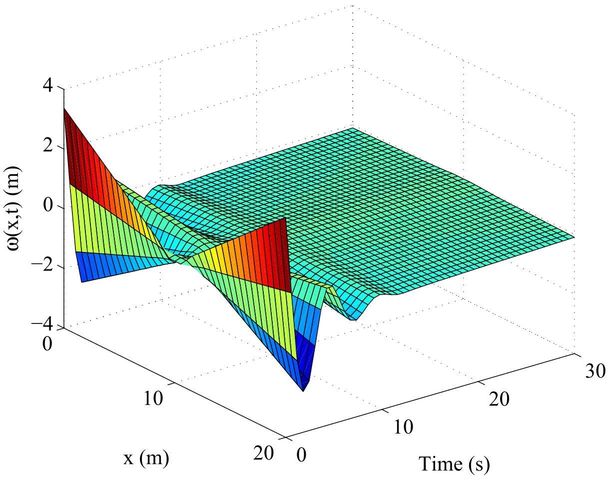

FIGURE 4. Deflection of the spacecraft with the proposed boundary control laws.

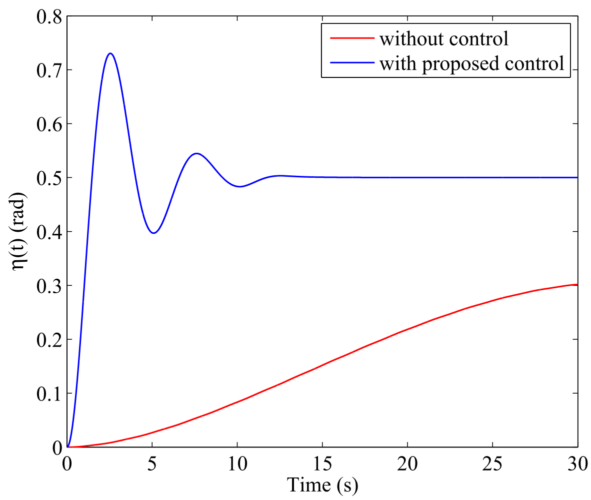

FIGURE 5. Angular position of the spacecraft with the proposed boundary control laws.

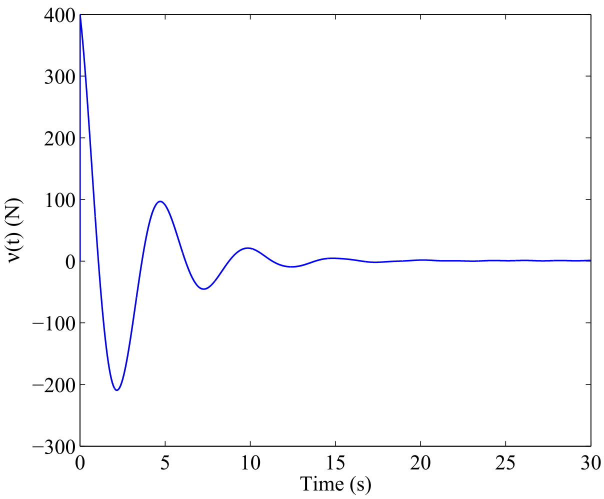

FIGURE 6. Designed control torque.

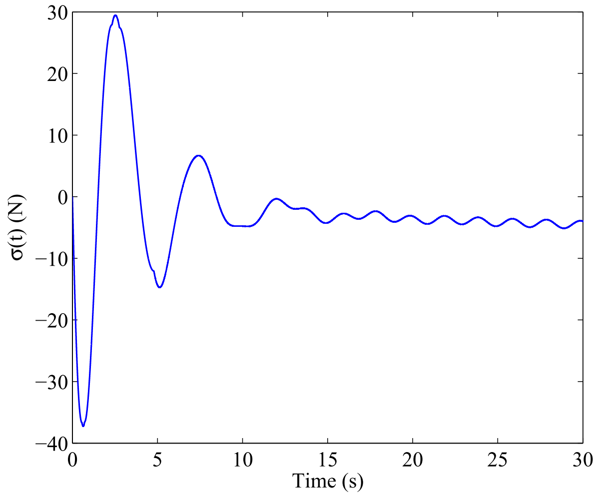

FIGURE 7. Designed control force.

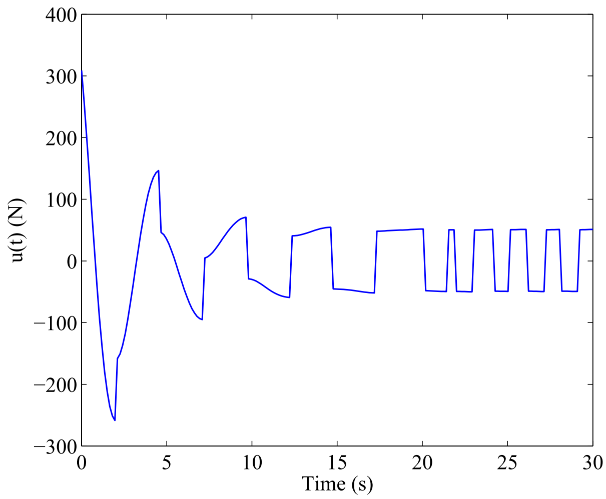

FIGURE 8. Actual control torque.

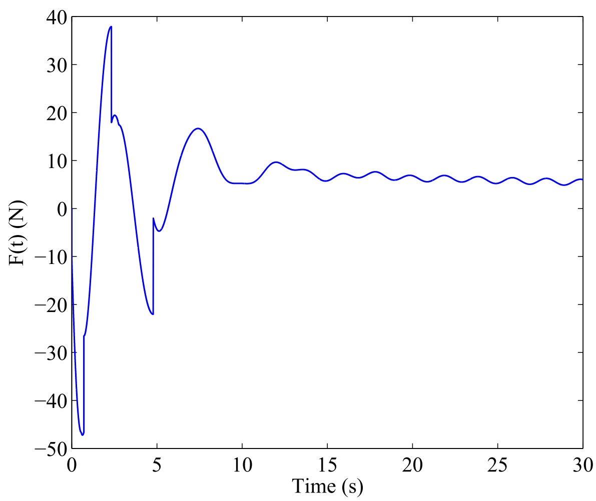

FIGURE 9. Actual control force.

Figs. 4 presents that the developed control can suppress the vibrational deflection to zero by the proposed controls in about 15s. As is shown in 5, thanks to the control schemes, the angle displacement is regulated to 0.5rad in less than 15 seconds. The desired control commands $\nu(t)$ and $\sigma(t)$ are bounded and smooth as demonstrated in Fig. 6 and Fig. 7.

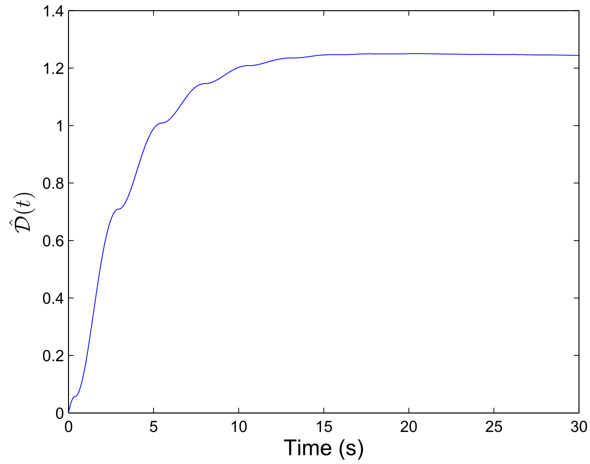

FIGURE 10. Online updating law $\hat{\mathcal{D}}(t)$.

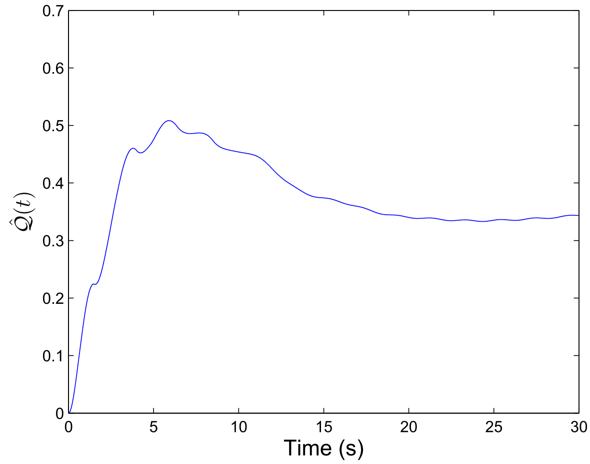

FIGURE 11. Online updating law $\hat{\mathcal{Q}}(t)$.

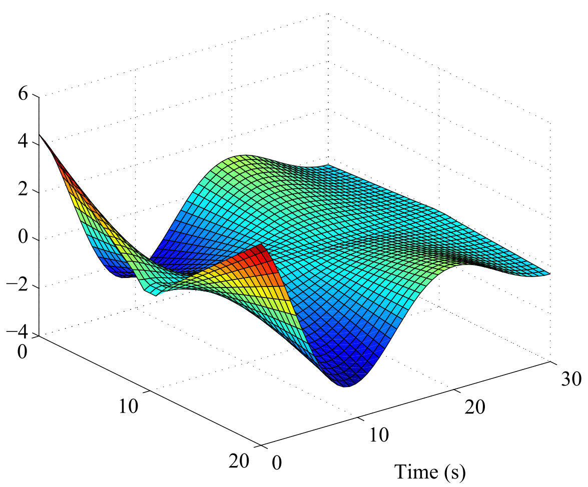

FIGURE 12. Deflection of the spacecraft with PD controls.

Moreover, the performances of the actual controls and the adaptive laws are illustrated in Figs. 8, 7, 10 and 11.

As a comparison, we replace the control laws (21) and (22) with classical PD controls, namely, $\nu_{PD} = -k_{p1}\eta(t) - k_{d1}\dot{\eta}(t)$ and $\sigma_{PD} = -k_{p1}\omega(l,t) - k_{d1}\dot{\omega}(l,t)$, respectively, where $k_{p1} = 10$, $k_{d1} = 6$, $k_{p2} = 100$ and $k_{d2} = 80$. As shown in Fig. 12, the offset can be stabilized near to zero slowly.

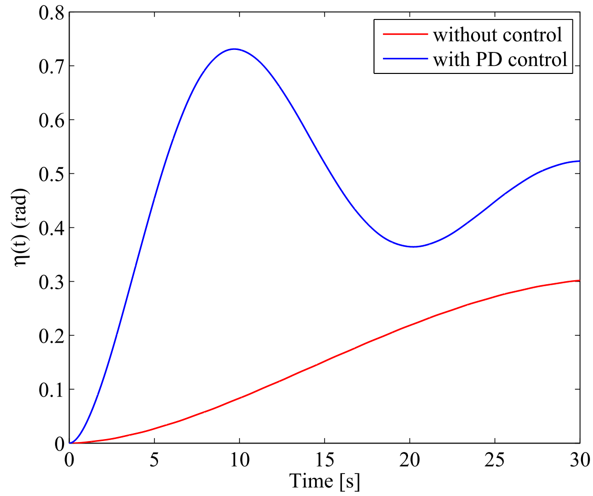

FIGURE 13. Angular position of the spacecraft with PD controls.

From Fig. 13, the angle displacement cannot be regulated to the desired position, but the bias is tapering off and close to 0.5 rad at the 30s. Hence, we can conclude that by employing the PD control laws, the flexible spacecraft system is stabilized to some extent. However, the control result is inferior to ours.

Therefore, the above simulations suggest that the proposed novel control scheme in this paper can handle the unknown backlash and prove the ultimately uniform stability of the closed-loop system.

V. CONCLUSION

In this study, the vibration suppression issue for a flexible spacecraft system subject to unknown external disturbance and uncertain input backlash non-linearity was addressed. The backlash error and external disturbance were reformulated as a combined "disturbance like" item. The upper-bound of a such item was estimated by designing a proper online updating law. Two adaptive vibration control inputs were constructed for eliminated the effect of the "disturbance like" items. With the boundary control schemes, the stabilization of the spacecraft's offset was achieved and the angle positions were regulated in the desired region. Numerical simulations were performed to illustrate the performance of the control designed. A further research is conducted the work of this paper into a 3-DOF attitude described flexible spacecraft model.

APPENDIX A
PROOF OF LEMMA 1

According to (29) and (30), we have

$$\delta_1[e^2 + \dot{e}^2 + \int_0^l [Y_{L_e}^2(x,t)dx + \dot{Y}_L^2(x,t)]dx + \int_l^{2l} [Y_{R_e}^2(x,t) + \dot{Y}_R^2(x,t)]dx] \leq \mathcal{V}_a(t) + \mathcal{V}_b(t) \quad (41)$$

where $2\delta_1 = \max\{\beta\gamma_1, \alpha\rho, \alpha k_2 + \beta k_1, \alpha I_h\}$.

Moreover, from (31) we obtain

$$|\mathcal{V}_c(t)| \leq \frac{\beta I_h}{2}(e+\dot{e}) + \frac{\beta\rho}{2}[\int_0^l [Y_{L_e}^2(x,t)dx + \dot{Y}_L^2(x,t)]dx + \int_l^{2l} [Y_{R_e}^2(x,t) + \dot{Y}_R^2(x,t)]dx]] \leq \delta_2(\mathcal{V}_a(t)+\mathcal{V}_b(t)) \tag{42}$$

where $\delta_2 = \beta\max\{I_h,\rho\}/2\delta_1$. It implies that

$$-\delta_2[\mathcal{V}_a(t)+\mathcal{V}_b(t)] \leq \mathcal{V}_c(t) \leq \delta_2[\mathcal{V}_a(t)+\mathcal{V}_b(t)]. \tag{43}$$

We choose a proper $0 < \beta < 2\delta_1/\max\{I_h,\rho\}$ for getting $0 < \mu_1 = 1-\delta_2 < 1$, then we have

$$0 \leq \lambda_1[\mathcal{V}_a(t)+\mathcal{V}_b(t)+\tilde{\mathcal{D}}^2(t)+\tilde{\mathcal{Q}}^2(t)] \leq \mathcal{V}(t) \leq \lambda_2[\mathcal{V}_a(t)+\mathcal{V}_b(t)+\tilde{\mathcal{D}}^2(t)+\tilde{\mathcal{Q}}^2(t)] \tag{44}$$

where $\lambda_1 = \min\{\mu_1, \frac{1}{2}\}$ and $\lambda_2 = 1+\delta_1 > 1$. □

APPENDIX B
PROOF OF LEMMA 2

Differentiating (28) leads to

$$\dot{\mathcal{V}}(t) = \dot{\mathcal{V}}_a(t)+\dot{\mathcal{V}}_b(t)+\dot{\mathcal{V}}_c(t)+\tilde{\mathcal{D}}(t)\dot{\tilde{\mathcal{D}}}(t)+\tilde{\mathcal{Q}}(t)\dot{\tilde{\mathcal{Q}}}(t). \tag{45}$$

$$\begin{aligned}\dot{\mathcal{V}}_a(t) = {}& \alpha EI\int_0^l \omega_L''(x,t)\dot{\omega}_L''(x,t)dx + \alpha EI\int_l^{2l} \omega_R''(x,t)\dot{\omega}_R''(x,t)dx \\ &+ \beta\gamma_1\int_0^l Y_{L_e}(x,t)\dot{Y}_{L_e}(x,t)dx + \beta\gamma_1\int_l^{2l} Y_{R_e}(x,t)\dot{Y}_{R_e}(x,t)dx \\ &+ \alpha\rho\int_0^l \dot{Y}_L(x,t)\ddot{Y}_L(x,t)dx + \alpha\rho\int_l^{2l} \dot{Y}_R(x,t)\ddot{Y}_R(x,t)dx.\end{aligned} \tag{46}$$

Substituting governing equations (2) and using integration by parts, we have

$$\begin{aligned}\dot{\mathcal{V}}_a(t) \leq {}& -\alpha\gamma_1\int_0^l \dot{Y}_L^2(x,t)dx - \alpha\gamma_1\int_l^{2l}\dot{Y}_R^2(x,t)dx \\ &- \alpha EI[\omega_R''(l,t)-\omega_L''(l,t)]\dot{e} \\ &- \alpha EI[\omega_L'''(l,t)-\omega_R'''(l,t)]\dot{\omega}(l,t) \\ &+ \beta\gamma_1\int_0^l Y_{L_e}(x,t)\dot{Y}_{L_e}(x,t)dx \\ &+ \beta\gamma_1\int_l^{2l} Y_{R_e}(x,t)\dot{Y}_{R_e}(x,t)dx.\end{aligned} \tag{47}$$

Taking the time derivative for $\mathcal{V}_b(t)$, we have

$$\dot{\mathcal{V}}_b(t) = \alpha m u_a(t)\dot{u}_a(t) + \alpha k_d\omega(l,t)\dot{\omega}(l,t) + (\beta k_1+\alpha k_2)e\dot{e} + \alpha I_h\dot{e}\ddot{e}. \tag{48}$$

Applying (26), (18) and (22), we obtain

$$\begin{aligned}\alpha m u_a(t)\dot{u}_a(t) = {}& -\alpha k u_a^2(t) - k_d\omega(l,t)\dot{\omega}(l,t) - \beta k_d\omega^2(l,t) \\ &+ \alpha EI u_a(t)[\omega_L'''(l,t)-\omega_R'''(l,t)] \\ &+ \alpha u_a(t)[-\tanh(u_a(t))\hat{\mathcal{Q}}(t)+d_2(t)].\end{aligned} \tag{49}$$

Moreover, using (17) and (21), we have

$$\alpha I_h\dot{e}\ddot{e} = \alpha\dot{e}EI[\omega_R''(l,t)+\omega_L''(l,t)] - \alpha k_1\dot{e}^2 - \alpha k_2 e\dot{e} + \alpha\dot{e}[-\tanh(h(t))\hat{\mathcal{D}}(t)+d_1(t)]. \tag{50}$$

Substituting (49) and (50) into (48), we have

$$\begin{aligned}\dot{\mathcal{V}}_b(t) \leq {}& -\alpha k u_a^2(t) - \beta k_d\omega^2(l,t) - \alpha k_1\dot{e}^2 + \beta k_1 e\dot{e} \\ &+ \alpha\dot{e}EI[\omega_R''(l,t)+\omega_L''(l,t)] \\ &+ \alpha EI u_a(t)EI[\omega_L'''(l,t)-\omega_R'''(l,t)] \\ &- \alpha\dot{e}\tanh(h(t))\hat{\mathcal{D}}(t) + \alpha\dot{e}d_1(t) \\ &- \alpha u_a(t)\tanh(u_a(t))\hat{\mathcal{Q}}(t) + \alpha u_a(t)d_2(t).\end{aligned} \tag{51}$$

For the third term of (45), we have

$$\begin{aligned}\dot{\mathcal{V}}_c(t) = {}& \beta I_h\dot{e}^2 + \beta I_h e\ddot{e} \\ &+ \beta\rho[\int_0^l \ddot{Y}_L(x,t)Y_{L_e}(x,t)dx + \int_0^l \dot{Y}_L^2(x,t)dx \\ &+ \int_l^{2l}\ddot{Y}_R(x,t)Y_{R_e}(x,t)dx + \int_l^{2l}\dot{Y}_R^2(x,t)dx].\end{aligned} \tag{52}$$

Substituting (3) and (21), we have

$$\beta I_h\ddot{e}e = \beta EI[\omega_R''(l,t)-\omega_L''(l,t)]e - \beta k_1\dot{e}e - \beta k_2 e^2 - \beta e[\tanh(h(t))\hat{\mathcal{D}}(t)+d_1(t)]. \tag{53}$$

Applying (2) and using integration by parts yield

$$\begin{aligned}&\beta\rho\int_0^l \ddot{Y}_L(x,t)Y_{L_e}(x,t)dx \\ &= -\beta\gamma_1\int_0^l \dot{Y}_L(x,t)Y_{L_e}(x,t)dx - \beta EI[\omega_L'''(l,t)\omega(l,t) \\ &\quad - \omega_L''(l,t)e + \int_0^l [\omega_L''(x,t)]^2dx]\end{aligned} \tag{54}$$

and

$$\begin{aligned}&\beta\rho\int_l^{2l} \ddot{Y}_R(x,t)Y_{R_e}(x,t)dx \\ &= -\beta\gamma_1\int_l^{2l} \dot{Y}_R(x,t)Y_{R_e}(x,t)dx - \beta EI[-\omega_R'''(l,t)\omega(l,t) \\ &\quad + \omega_R''(l,t)e + \int_l^{2l}[\omega_R''(x,t)]^2dx].\end{aligned} \tag{55}$$

Therefore, we obtain

$$\begin{aligned}&\dot{\mathcal{V}}_c(t) \\ &\leq \beta I_h\dot{e}^2 - \beta k_1 e\dot{e} - \beta k_2 e^2 \\ &\quad + \beta\rho[\int_0^l \dot{Y}_L^2(x,t)dx + \int_l^{2l}\dot{Y}_R^2(x,t)dx] \\ &\quad - \beta\gamma_1[\int_0^l \dot{Y}_L(x,t)Y_{L_e}(x,t)dx \\ &\quad + \int_l^{2l}\dot{Y}_R(x,t)Y_{R_e}(x,t)dx] \\ &\quad - \beta EI[\omega_L'''(l,t)-\omega_R'''(l,t)]\omega(l,t)\end{aligned}$$

$$- \beta EI[\int_0^l [\omega_L''(x,t)]^2 dx + \int_l^{2l} [\omega_R''(x,t)]^2 dx] - \beta e[\tanh(h(t))\hat{\mathcal{D}}(t) + d_1(t)] \quad (56)$$

according to (52), (53), (54) and (55).

Applying (12), (23), (24)and (25), we further have

$$-\alpha\dot{e}\tanh(h(t))\hat{\mathcal{D}}(t) + \alpha\dot{e}d_1(t) - \alpha u_a(t)\tanh(u_a(t))\hat{\mathcal{Q}}(t) + \alpha u_a(t)d_2(t) - \beta e\tanh(h(t))\hat{\mathcal{D}}(t) - \beta e\tanh(h(t))d_1(t) + \tilde{\mathcal{D}}(t)\dot{\hat{\mathcal{D}}}(t) + \tilde{\mathcal{Q}}(t)\dot{\hat{\mathcal{Q}}}(t) \le \frac{\xi_1}{2}\mathcal{D}^2 - \frac{\xi_1}{2}\tilde{\mathcal{D}}^2(t) + \frac{\xi_2}{2}\mathcal{Q}^2 - \frac{\xi_2}{2}\tilde{\mathcal{Q}}^2(t). \quad (57)$$

By the boundary conditions (4), the following inequality holds

$$J[\int_0^l Y_{L_e}^2(x,t)dx + \int_l^{2l} Y_{R_e}^2(x,t)dx] \le 4Jl\omega^2(l,t) + 16Jl^3e^2 + 16Jl^4[\int_0^l [\omega_L''(x,t)]^2 dx + \int_l^{2l} [\omega_R''(x,t)]^2 dx] \quad (58)$$

where J is a positive constant.

Together all of (47), (51), (56), (57) and (58), we have

$$\dot{\mathcal{V}}(t) \le -(\alpha\gamma_1 - \beta\rho)[\int_0^l \dot{Y}_L^2(x,t)dx + \int_0^l \dot{Y}_R^2(x,t)dx] - J[\int_0^l Y_{L_e}^2(x,t) + \int_l^{2l} Y_{R_e}^2(x,t)] - (\beta EI - 16Jl^4)[\int_0^l [\omega_L''(x,t)]^2 dx + \int_l^{2l} [\omega_R''(x,t)]^2 dx] - \alpha k u_a^2(t) - (\beta k_d - 4Jl)\omega^2(l,t) - (\alpha k_1 - \beta I_h)\dot{e}^2 - (\beta k_2 - 16Jl^3)e^2 \frac{\xi_1}{2}\mathcal{D}^2 - \frac{\xi_1}{2}\tilde{\mathcal{D}}^2(t) + \frac{\xi_2}{2}\mathcal{Q}^2 - \frac{\xi_2}{2}\tilde{\mathcal{Q}}^2(t). \quad (59)$$

Carefully choosing proper parameters $\alpha,\ \beta,\ J,\ k,\ k_d\ k_1\ k_2$ and let them satisfy the following conditions

$$\alpha\gamma_1 - \beta\rho > 0 \quad (60)$$
$$\beta EI - 16Jl^4 > 0 \quad (61)$$
$$\beta k_d - 4Jl > 0 \quad (62)$$
$$\alpha k_1 - \beta I_h > 0 \quad (63)$$
$$\beta k_2 - 16Jl^3 > 0. \quad (64)$$

Then we have

$$\dot{\mathcal{V}}(t) \le -\lambda_3[\mathcal{V}_a(t) + \mathcal{V}_b(t) + \tilde{\mathcal{D}}^2(t) + \tilde{\mathcal{Q}}^2(t)] + \varepsilon \quad (65)$$

where

$$\lambda_3 = \min\{\frac{2(\alpha\gamma_1 - \beta\rho)}{\alpha\rho}, \frac{2J}{\beta\gamma_1}, \frac{2(\beta EI - 16Jl^4)}{\alpha EI}, \frac{2k}{m}, \frac{2(\beta k_d - 4Jl)}{\alpha k_d}, \frac{2(\alpha k_1 - \beta I_h)}{\alpha I_h}, \frac{2(\beta k_2 - 16Jl^3)}{\alpha k_2 + \beta k_1}, \xi_1, \xi_2\} > 0 \quad (66)$$

and

$$\varepsilon = \frac{\xi_1}{2}\mathcal{D}^2 + \frac{\xi_2}{2}\mathcal{Q}^2. \quad (67)$$

Therefore, combining (32) and (59), we get

$$\dot{\mathcal{V}}(t) \le -\lambda\mathcal{V}(t) + \varepsilon \quad (68)$$

where $\lambda = \lambda_3/\lambda_2$ and $\varepsilon > 0$. □

REFERENCES

[1] J. Zhou and C. Wen, *Adaptive Backstepping Control of Uncertain Systems Nonsmooth Nonlinearities, Interactions or Time-Variations*. New York, NY, USA: Springer, 2008.

[2] Z. Zhao, J. Shi, X. Lan, X. Wang, and J. Yang, "Adaptive neural network control of a flexible string system with non-symmetric dead-zone and output constraint," *Neurocomputing*, vol. 283, pp. 1–8, Mar. 2018.

[3] J. Yao and W. Deng, "Active disturbance rejection adaptive control of uncertain nonlinear systems: Theory and application," *Nonlinear Dyn.*, vol. 89, no. 3, pp. 1611–1624, May 2017.

[4] Z. J. Zhao, X. Y. He, and G. L. Wen, "Boundary robust adaptive anti-saturation control of vibrating flexible riser systems," *Ocean Eng.*, vol. 179, pp. 298–306, May 2019.

[5] M. Chen, Y. Ren, and J. Liu, "Antidisturbance control for a suspension cable system of helicopter subject to input nonlinearities," *IEEE Trans. Syst., Man, Cybern. Syst.*, vol. 48, no. 12, pp. 2292–2304, Dec. 2018.

[6] F. Guo, Y. Liu, and F. Luo, "Adaptive stabilisation of a flexible riser by using the Lyapunov-based barrier backstepping technique," *IET Control Theory Appl.*, vol. 11, no. 14, pp. 2252–2260, 2017.

[7] J. Zhou, C. Wen, and Y. Zhang, "Adaptive backstepping control of a class of uncertain nonlinear systems with unknown backlash-like hysteresis," *IEEE Trans. Autom. Control*, vol. 49, no. 10, pp. 1751–1759, Oct. 2004.

[8] G. Tao and P. V. Kokotović, "Adaptive control of plants with unknown hystereses," *IEEE Trans. Autom. Control*, vol. 40, no. 2, pp. 200–212, Feb. 1995.

[9] S. Zhang, W. He, and D. Huang, "Active vibration control for a flexible string system with input backlash," *IET Control Theory Appl.*, vol. 10, no. 7, pp. 800–805, Apr. 2016.

[10] M. Nordin, J. Galic, and P.-O. Gutman, "New models for backlash and gear play," *Int. J. Adapt. Control Signal Process.*, vol. 11, no. 1, pp. 49–63, 1997.

[11] A. Müller, "Internal preload control of redundantly actuated parallel manipulators—Its application to backlash avoiding control," *IEEE Trans. Robot.*, vol. 21, no. 4, pp. 668–677, Aug. 2005.

[12] R. R. Selmic and F. L. Lewis, "Backlash compensation in nonlinear systems using dynamic inversion by neural networks," *Asian J. Control*, vol. 2, no. 2, pp. 76–87, 2000.

[13] H. Logemann, E. P. Ryan, and I. Shvartsman, "Integral control of infinite-dimensional systems in the presence of hysteresis: An input-output approach," *ESAIM, Control, Optim. Calculus Variat.*, vol. 13, no. 3, pp. 458–483, 2007.

[14] A. Esbrook, X. Tan, and H. K. Khalil, "Inversion-free stabilization and regulation of systems with hysteresis via integral action," *Automatica*, vol. 50, no. 4, pp. 1017–1025, 2014.

[15] W. He, X. He, M. Zou, and H. Li, "PDE model-based boundary control design for a flexible robotic manipulator with input backlash," *IEEE Trans. Control Syst. Technol.*, vol. 27, no. 2, pp. 790–797, Mar. 2018.

[16] Q. Hu and G. Ma, "Variable structure control and active vibration suppression of flexible spacecraft during attitude maneuver," *Aerosp. Sci. Technol.*, vol. 9, no. 4, pp. 307–317, Jun. 2005.

[17] Q. Hu, "Neural network-based adaptive attitude tracking control for flexible spacecraft with unknown high-frequency gain," *Int. J. Adapt. Control Signal Process.*, vol. 24, no. 6, pp. 477–489, Jun. 2010.

[18] M. Xin and H. Pan, "Integrated nonlinear optimal control of spacecraft in proximity operations," *Int. J. Control*, vol. 83, no. 2, pp. 347–363, Mar. 2010.

[19] S.-C. Lo and Y.-P. Chen, "Smooth sliding-mode control for spacecraft attitude tracking maneuvers," *J. Guid., Control, Dyn.*, vol. 18, no. 6, pp. 1345–1349, Nov. 1995.

[20] C. C. Won, J. L. Sulla, D. W. Sparks, and W. K. Belvin, "Application of piezoelectric devices to vibration suppression," *J. Guid., Control, Dyn*, vol. 17, no. 6, pp. 1333–1338, Nov. 1994.

[21] S. Wu and S. Wen, "Robust H_∞ output feedback control for attitude stabilization of a flexible spacecraft," *Nonlinear Dyn.*, vol. 84, no. 1, pp. 405–412, 2016.
[22] J. Yao and W. Deng, "Active disturbance rejection adaptive control of hydraulic servo systems," *IEEE Trans. Ind. Electron.*, vol. 64, no. 10, pp. 8023–8032, Oct. 2017.
[23] Q. Hu, "Adaptive output feedback sliding-mode manoeuvring and vibration control of flexible spacecraft with input saturation," *IET Control Theory Appl.*, vol. 2, no. 6, pp. 467–478, Jun. 2008.
[24] Z. Zhao, X. Wang, C. Zhang, Z. Liu, and J. Yang, "Neural network based boundary control of a vibrating string system with input deadzone," *Neurocomputing*, vol. 275, pp. 1021–1027, Jan. 2018.
[25] C. Sun, W. He, and J. Hong, "Neural network control of a flexible robotic manipulator using the lumped spring-mass model," *IEEE Trans. Syst., Man, Cybern., Syst.*, vol. 47, no. 8, pp. 1863–1874, Aug. 2017.
[26] W. He, Y. Ouyang, and J. Hong, "Vibration control of a flexible robotic manipulator in the presence of input deadzone," *IEEE Trans. Ind. Informat.*, vol. 13, no. 1, pp. 48–59, Feb. 2017.
[27] J.-L. Wang, H.-N. Wu, and L. Guo, "Novel adaptive strategies for synchronization of linearly coupled neural networks with reaction-diffusion terms," *IEEE Trans. Neural Netw. Learn. Syst.*, vol. 25, no. 2, pp. 429–440, Feb. 2014.
[28] B. Xu, D. Wang, Y. Zhang, and Z. Shi, "DOB-based neural control of flexible hypersonic flight vehicle considering wind effects," *IEEE Trans. Ind. Electron.*, vol. 64, no. 11, pp. 8676–8685, Nov. 2017.
[29] M. Krstic and A. Smyshlyaev, *Boundary Control PDEs: A Course Backstepping Designs*. Philadelphia, PA, USA: SIAM, 2008, vol. 16.
[30] Z. Zhao, Z. Liu, Z. Li, N. Wang, and J. Yang, "Control design for a vibrating flexible marine riser system," *J. Franklin Inst.*, vol. 354, no. 18, pp. 8117–8133, 2017.
[31] P. Qi, X. Zhao, Y. Wang, R. Palacios, and A. Wynn, "Aeroelastic and trajectory control of high altitude long endurance aircraft," *IEEE Trans. Aerosp. Electron. Syst.*, vol. 54, no. 6, pp. 2992–3003, Dec. 2018.
[32] Z. Zhao, X. He, Z. Ren, and G. Wen, "Output feedback stabilization for an axially moving system," *IEEE Trans. Syst., Man, Cybern. Syst.*, to be published. doi: 10.1109/TSMC.2018.2882822.
[33] Q. C. Nguyen and K.-S. Hong, "Asymptotic stabilization of a nonlinear axially moving string by adaptive boundary control," *J. Sound Vibrat.*, vol. 329, no. 22, pp. 4588–4603, 2010.
[34] D. Liu, L. Zhang, and G. Xu, "Stabilisation of timoshenko beam system with a tip payload under the unknown boundary external disturbances," *Int. J. Control*, vol. 88, no. 9, pp. 1830–1840, Sep. 2015.
[35] J. Dai and B. Ren, "Ude-based robust boundary control for an unstable parabolic PDE with unknown input disturbance," *Automatica*, vol. 93, pp. 363–368, Jul. 2018.
[36] W. He and S. S. Ge, "Dynamic modeling and vibration control of a flexible satellite," *IEEE Trans. Aerosp. Electron. Syst.*, vol. 51, no. 2, pp. 1422–1431, Apr. 2015.
[37] Y. Liu, Y. Fu, W. He, and Q. Hui, "Modeling and observer-based vibration control of a flexible spacecraft with external disturbances," *IEEE Trans. Ind. Electron.*, to be published. doi: 10.1109/TIE.2018.2884172.
[38] H. K. Rad, H. Salarieh, A. Alasty, and R. Vatankhah, "Boundary control of anti-symmetric vibration of satellite with flexible appendages in planar motion with exponential stability," *Acta Astronautica*, vol. 147, pp. 219–230, Jan. 2018.
[39] Y. Fu, Y. Liu, and D. Huang, "Boundary output feedback control of a flexible spacecraft system with input constraint," *IET Control Theory Appl.*, vol. 12, no. 5, pp. 571–581, 2017.
[40] N. Ji and J. Liu, "Vibration control for a flexible satellite with input constraint based on nussbaum function via backstepping method," *Aerosp. Sci. Technol.*, vol. 77, pp. 563–572, Aug. 2018.
[41] Z. Zhao, X. He, Z. Ren, and G. Wen, "Boundary adaptive robust control of a flexible riser system with input nonlinearities," *IEEE Trans. Syst., Man, Cybern. Syst.*, to be published. doi: 10.1109/TSMC.2018.2882734.
[42] Z. Zhao, S. Lin, D. Zhu, and G. Wen, "Vibration control of a riser-vessel system subject to input backlash and extraneous disturbances," *IEEE Trans. Circuits Syst. II, Exp. Briefs*, to be published. doi: 10.1109/TCSII.2019.2914061.
[43] G. D. Smith, *Numerical Solution of Partial Differential Equations: Finite Difference Methods*. New York, NY, USA: Oxford Univ. Press, 1985.

ZHIQIANG LIN received the B.Eng. and M.Eng. degrees from South China Normal University, Guangzhou, China, in 2007 and 2010, respectively, and the Ph.D. degree from Guangzhou University, Guangzhou, in 2014. He held a postdoctoral position with the Institute of Information Engineering, Chinese Academy of Sciences, China, from 2014 to 2016. He is currently a Lecturer with Guangzhou University. His research interests include distributed parameter system control and cryptology.

SHIMIN LIN received the B.Sc. degree in computer science from The Chinese University of Hong Kong. She is currently pursuing the master's degree with the University of California at San Diego, San Diego, CA, USA. Her research interests include machine learning and robotics.

SEN WU is currently pursuing the degree with Guangzhou University. His research interests include robotics and vibration control.

GE MA received the B.S. degree in information and computing science from Shandong Jianzhu University, Jinan, China, in 2010, and the Ph.D. degree in automatic control from the South China University of Technology, Guangzhou, China, in 2016. She is currently a Lecturer with Guangzhou University. Her research interests include computer vision, robotics, and automatic control.

ZHONGWEI LIANG received the B.S. and M.S. degrees in mechatronic engineering from the Shenyang University of Technology, China, in 2000 and 2005, respectively, and the Ph.D. degree in machinery manufacturing and automation from the South China University of Technology, China, in 2008. He served as an Academic Research Fellow and a Visiting Research Professor with Zhejiang University, China, The University of New South Wales, Australia, and Northwestern University, USA, from 2014 to 2018. He is currently a Professor with Guangzhou University. His research interests include manufacturing mechanics of AWJ grinding, strengthen grinding, turbulence modeling, fluid mechanics, advanced manufacturing technology, and so on.